HHS Public Access

Author manuscript

Kidney Int. Author manuscript; available in PMC 2015 August 01.

Published in final edited form as:

Kidney Int. 2015 February ; 87(2): 382–395. doi:10.1038/ki.2014.286.

Reduced Krüppel-like Factor 2 expression may aggravate the endothelial injury of diabetic nephropathy

Fang Zhong[1,2], **Habing Chen**[1,3], **Chengguo Wei**[1], **Weijia Zhang**[1], **Zhengzhe Li**[1], **Mukesh K Jain**[5], **Peter Y. Chuang**[1], **Hongyu Chen**[2], **Yongjun Wang**[2], **Sandeep K. Mallipattu**[4], and **John Cijiang He**[1,6]

[1]Department of Medicine/Nephrology, Icahn School of Medicine at Mount Sinai, New York, NY

[2]Department of Nephrology; Hang Zhou Hospital of Traditional Chinese Medical, Zhejiang Chinese Medical University, China

[3]Department of Nephrology, Shanghai Six Municipal Hospital, Shanghai Jiaotao University School of Medicine

[4]Division of Nephrology, Department of Medicine, Stony Brook University, Stony Brook, NY

[5]Case Cardiovascular Institute Research Institute, Department of Medicine, Case Western Reserve University, Cleveland Ohio

[6]Renal Section, James J Peters VAMC, Bronx, NY

Abstract

Kruppel-like Factor 2 (KLF2), a shear-stress inducible transcription factor, has endoprotective effects. In streptozotocin-induced diabetic rats, we found that glomerular *Klf2* expression was reduced in comparison to non-diabetic rats. However, normalization of hyperglycemia by insulin treatment increased *Klf2* expression to a level higher than that of non-diabetic rats. Consistent with this, we found that Klf2 expression was suppressed by high glucose but increased by insulin in cultured endothelial cells. To determine the role of KLF2 in streptozotocin-induced diabetic nephropathy, we used endothelial cell-specific *Klf2* heterozygous knockout mice and found that diabetic knockout mice developed more kidney/glomerular hypertrophy and proteinuria than diabetic wide type mice. Glomerular expression of *Vegfa*, *Flk1*, and *angiopoietin 2* increased but expression of *Flt1*, *Tie2*, and *angiopoietin 1* decreased in diabetic knockout compared to diabetic wide type mice. Glomerular expression of ZO-1, glycocalyx, and eNOS was also decreased in diabetic knockout compared to diabetic wide type mice. These data suggest knockdown of Klf2 expression in the endothelial cells induced more endothelial cell injury. Interestingly, podocyte

Corresponding author: John Cijiang He, MD Division of Nephrology, Box 1243 Mount Sinai School of Medicine One Gustave L Levy Place New York NY 10029 Tel: 212-659-1703, Fax: 212-987-0389 cijiang.he@mssm.edu.

Author contributions:

FZ, CH, SM, and LZ performed experiments and WC and ZW performed data analysis. JM provided Klf2 floxed mice. JCH, FZ, HYC, YJW, PC, and SM designed experimental and wrote the paper.

Conflict of Interest:

The authors declare that they have no competing financial interests.

injury was also more prominent in diabetic knockout compared to diabetic wide type mice, indicating a crosstalk between these two cell types. Thus, KLF2 may play a role in glomerular endothelial cell injury in early diabetic nephropathy.

Keywords

diabetic nephropathy; endothelium; podocyte

Introduction

Diabetic nephropathy (DN) is a serious and common complication of both type 1 and type 2 diabetes, leading to end-stage renal disease (ESRD) (1). The current management with tight glycemic control and inhibition of renin angiotensin system (RAS) reduces the incidence and slows the progression of DN (1). However, the prevalence of DN remains high and many patients on RAS inhibitors still progress to ESRD. Therefore, there is an urgent need to develop more effective therapies for this disease. Elucidating mechanisms that mediate the early stage of DN may help us identify novel preventive and therapeutic measures for patients with DN.

The early stage of DN is characterized by glomerular hyperfiltration and hypertrophy (2). Podocyte injury, as a result of cell detachment and apoptosis has been described to be an early event in DN (3). Recent evidence suggests that glomerular endothelial cell injury is a critical pathological process at the early stage of DN (4). In the glomerulus, vascular endothelial growth factor-A (VEGF)-induced neoangiogenesis may contribute to the initial hyperfiltration and microalbuminuria due to the increased filtration area and immaturity of the neovessels (4). In addition, reduced nitric oxide levels also plays a critical role in the development of DN through disruption of glomerular autoregulation, uncontrolled VEGF action, and release of prothrombotic substances by endothelial cells (5) (6) (7). Also, thrombomodulin-dependent activated protein C (APC) formation has been shown to mediate cytoprotection in DN by inhibiting glomerular endothelial and podocyte apoptosis (8). Furthermore, disturbances in endothelial glycocalyx may also contribute to disturbances in permselectivity and microalbuminuria (9) (10). Finally, a podocyte-endothelial cross talk has been elegantly characterized in the context of elevated profibrotic cytokine transforming growth factor-β levels (11).

Krüppel-like Factors (KLFs) are a subfamily of 17 DNA-binding transcriptional regulators that are involved in a broad range of cellular processes, such as cell differentiation, angiogenesis, erythropoiesis, and immune regulation (12), (13-17). KLF2 is an essential regulator of vascular hemodynamic forces *in vivo* (18) and mediates flow-dependent phenotype in endothelial cells (12) (19). KLF2 has been described to exhibit protective effects in endothelial cells by regulation of endothelial pro-inflammatory pathway, thrombotic activation, cell proliferation and migration, and angiogenesis (20). In addition, Klf2 is essential to the maintenance of endothelial integrity in adult mice (21) as well as in mouse embryonic vasculature (22). KLF2 inhibits VEGF-A-mediated angiogenesis (23) and

regulates endothelial thrombotic function (24). KLF2 also exhibits anti-inflammatory effects in endothelial cells, thereby protecting the cell from injury in the setting of stress (25).

To date, the role of KLF2 in kidney disease has not been well studied. The expression of KLF2 in the glomerulus is suppressed in renal transplant patients with thrombotic microangiopathy (26). In contrast, chronic exposure to laminar shear stress induces KLF2 expression in glomerular endothelial cells (27). One study suggests that KLF2 expression is suppressed in cultured endothelial cells exposed to high glucose medium (28). Based on these findings and the critical role of KLF2 in endothelial cells, we sought to determine whether the expression of KLF2 is regulated in glomeruli of diabetic kidney and whether KLF2 has a cytoprotective role against endothelial cell dysfunction in early DN.

RESULTS

Klf2 expression is regulated in glomeruli of rats with early DN

To examine the regulation of Klf2 in the early stage of DN, low-dose streptozotocin (STZ) was used to induce diabetes in rats. Gender and age-matched diabetic and wild type rats (n=5) were sacrificed at either 6 weeks or 12 weeks after the onset of diabetes. In addition, a separate group (n=5) of diabetic rats were treated with insulin to maintain tight glycemic control from week 6 to 12 and sacrificed at 12 weeks after the onset of diabetes. Body weight, blood glucose, renal weight/body weight, and urine albumin/creatinine were measured at the time of sacrifice (Supplementary table 1).

Glomeruli were isolated from kidneys of these rats by sieving method with >90% purity (29). Diabetic rats exhibited a 20-30% reduction of glomerular Klf2 mRNA level at both 6 and 12 weeks of diabetes. However, glomerular Klf2 mRNA level was significantly higher in diabetic rats treated with insulin than non-diabetic rats. A similar pattern of changes was observed for Klf2 protein expression in these rats by immunostaining (Supplementary figure 1). These data suggest that Klf2 expression is likely suppressed by hyperglycemia at the early stage of DN in rats. However, Klf2 expression was higher in diabetic rats than control rats after serum glucose normalization by insulin treatment, suggesting a potential role of insulin in the regulation of Klf2 expression.

High glucose decreases and insulin increases KLF2 expression in cultured endothelial cells

To confirm whether exposure to high glucose suppresses Klf2 expression in endothelial cells, HUVEC were incubated in either high glucose (30mM), or normal glucose (5mM) medium ± mannitol (25mM). As shown in Figure 1A-1C, incubation of HUVEC with high glucose (30mM) suppressed both KLF2 mRNA and protein expression as compared to cells incubated in normal glucose media (5mM) ± mannitol (25mM). In addition, we determined the effects of high glucose and insulin in human glomerular microvascular endothelial cells (Cell System, Kirkland, WA). In these cells, we confirmed that high glucose suppressed KLF2 mRNA and protein levels while insulin treatment stimulated its expression (Figure 1D-F). These data confirm that KLF2 expression in endothelial cells is regulated negatively by high glucose but positively by insulin.

KLF2 expression in human diabetic kidney

Most rodent models of DN, including STZ-induced DN in rats, are more representative of early stage of DN. Recent studies suggest a different or opposite patterns of renal gene expression profiles between diabetic animals and patients (30). Therefore, we sought to determine KLF2 expression in human diabetic kidney. By immunostaining, we found that KLF2 expression was reduced in glomerular cells of kidney biopsy samples from patients with DN as compared to normal kidney tissue from nephrectomy samples (Figure 2A, 2B). The clinical information of these patients is shown in the supplementary table 2. The staining was mostly nuclear and distributed in all glomerular cells as well as tubular epithelial cells. The quantification of the staining was shown in Figure 2C. These data suggest that KLF2 expression was significantly reduced in all glomerular cells and some reduction was also observed in tubular epithelial cells of human diabetic kidneys with advanced DN.

Generation of endothelial cell specific *Klf2* knockout mice using the *VE-Cadherin-Cre* Transgene

Since glomerular endothelial-specific Cre mice are not available, we developed global endothelial cell Klf2 knockout mice by crossing *klf2* floxed mice (18) with *VECCre* mice (from Jackson lab) (Supplementary Figure 2A). As previously described, homozygous *VEC-Cre/Klf2*$^{fl/fl}$ mice died embryonically (18). However, heterozygous *VEC-Cre/Klf2*$^{fl/+}$ mice are viable and healthy. Therefore, heterozygous *VEC-Cre/Klf2*$^{fl/+}$ mice (KO) and control *VEC-Cre/Klf2*$^{+/+}$ mice (WT) were used in this study. To confirm the reduction of Klf2 expression in glomerular endothelial cells, we isolated glomerular endothelial cells from KO mice (31) and determined *Klf2* expression by real-time PCR. We found that Klf2 mRNA was significantly reduced by 40-50% in endothelial cells isolated from KO mice as compared to WT mice. As the control, mRNA levels of Pecam- 1 and Icam-1 did not change between two groups (Supplementary Figure 2B). At baseline, proteinuria and kidney histological changes were not observed in KO mice when they were examined at both 6 months and 12 months of age (data not shown).

Diabetes induces more kidney injury in KO mice than WT mice

Eight-week old WT and KO mice were induced with diabetes by STZ injection. After STZ treatment, blood glucose levels were monitored every 2 weeks and were similar between WT-STZ and KO-STZ mice (Figure 3A). All mice were sacrificed at the age of 28 weeks, which was 20 weeks after STZ injection. Both WT-STZ and KO-STZ mice experienced similar weight loss as compared to non-diabetic mice (Figure 3B). Both WT-STZ and KO-STZ mice developed kidney hypertrophy, as measured by an increase in kidney weight to body weight ratio. However, KO-STZ mice had a significant increase in kidney hypertrophy as compared to WT-STZ mice (Figure 3C). A trend towards an increased blood pressure was observed in the diabetic mice as compared to non-diabetic mice but did not reach the statistical significance. In addition, there was no significant difference of blood pressure between KO and WT groups with or without diabetes (Figure 3D). In the KO mice, total glomerular Klf2 mRNA (Figure 4A) and protein expression (Figure 4B and 4C) were not significantly reduced as compared to WT mice (Figure 4A-4C) likely because Klf2 was

knocked out only in glomerular endothelial cells. WT-STZ mice exhibited a significant reduction in glomerular KLF2 mRNA compared to non-diabetic WT mice while reduction of KLF2 protein expression did not reach statistical significance probably due to the semi-quantitative nature of immunofluorescence staining. However, KO-STZ mice had significantly lower glomerular expression of Klf2 at both mRNA and protein levels compared to the mice in all other groups (Figure 4A-4C). A significant increase in albuminuria was observed earlier in the KO-STZ mice, starting at 6 weeks after STZ injection, whereas the WT- STZ mice developed an increase in albuminuria starting at 10 weeks after STZ injection. In addition, starting at 16 weeks after STZ injection, KO-STZ mice exhibited a significant increase in albuminuria compared to WT-STZ mice (Figure 5A). The increase in albuminuria was also confirmed by measuring total albumin in a 12-hour urine collection before the mice were sacrificed at 20 weeks after STZ injection (Figure 5B). Histological analysis revealed an increase in glomerular volume and mesangial matrix area in both WT-STZ and KO-STZ groups as compared with non-diabetic mice (Figure 6A-C). The glomerular area was significantly increased in KO-STZ mice than WT-STZ mice whereas the mesangial matrix area fraction was not significantly different between these two groups of mice (Figure 6B and 6C). In addition, we performed immunostaining of F4/80 to determine macrophage infiltration in diabetic kidneys of these mice and found that F4/80 staining was increased in WT-STZ mice compared to non-diabetic mice and a further increase was observed in KO-STZ mice compared to WT-STZ mice (Figure 6A and D).

Knockdown of Klf2 causes more injury to glomerular endothelial cells in diabetic mice

KLF2 is constitutively expressed in endothelial cells and has been described to have an endo-protective effect in the setting of cell stress (20). KLF2 also affects the expression of angiogenesis markers such as Flk1, Flt1, Angpt 1, Angpt 2, and Tie-2 (32). Furthermore, the expression of these genes is also altered in glomerular endothelial cells of diabetic kidneys (4). Therefore, we ascertained whether the knockdown of *Klf2* in endothelial cells affected the expression of these angiogenesis markers in diabetic mice. The mRNA levels of *Vegfa, Flk1*, *Angpt1*, and *Tie-2* were measured in the glomeruli isolated from these mice by real-time PCR. We determined that knockdown of *Klf2* expression in endothelial cells caused further increases of *Vegfa, Flk1*, and *Angpt2* in KO-STZ mice compared to WT-STZ mice. In contrast, the expression of *Flt1*, *Angpt1*, and *Tie-2* was further reduced in KO-STZ mice as compared to WT-STZ mice (Figure 7A). Previous studies have revealed that a reduction in endothelial glycocalyx leads to decreased permselectivity and microalbuminuria in DN (33) (9). Therefore, we examined the glycocalyx in these mice by immunostaining and observed that glycocalyx staining was significantly reduced in both WT-STZ and KO-STZ mice but a more dramatic reduction was only observed in KO-STZ mice (Figure 7B). KLF2 also plays a critical role in endothelial barrier function in adult mice by regulating expression of tight junction proteins (21). Consequently, we examined the expression of tight junction protein 1 (ZO-1) by both real-time PCR and immunofluorescence in the glomeruli from these mice. ZO-1 mRNA levels were reduced in diabetic mice compared to non-diabetic mice. However, a significant further reduction was observed in KO-STZ mice compared to WT-STZ mice (Figure 7C). For immunofluorescence, the staining of ZO-1 was quantified in glomeruli of these mice. A significant reduction of ZO-1/glomeruli staining was observed in KO-STZ mice compared to mice of other groups (Figure 7D and 7E). To

determine the specific staining of ZO-1 in glomerular endothelial cells we also quantified the areas with co-staining of ZO-1 and CD31. We found that the staining areas with both ZO-1/CD31 were significantly reduced in diabetic mice compared to non-diabetic mice but a further reduction was observed in KO-STZ compared to WT- STZ mice (Figure 7D and 7F).

Regulation of Klf2-target genes in glomeruli of diabetic mice

We conducted a transcription factor database search using TRANSFAC (http://www.gene-regulation.com/pub/databases.html) (34), JASPAR (http://jaspar.genereg.net/) (35), and MatBase (http://www.genomatix.de/index.html) (36) to identify genes directly targeted by Klf2 (Supplementary table 3). Nitric oxide synthase 3 (*Nos3*), which encode endothelial nitric oxide synthase (eNOS), was identified as a potential gene regulated by KLF2. Previous studies have characterized the critical role of eNOS in DN (5) (37) (38). In addition, we observed that both mRNA and protein levels of eNOS were significantly decreased in glomeruli of KO-STZ as compared to all other groups (Figure 8A-8C).

Podocyte injury in endothelial cell specific KO-STZ mice

Since KO-STZ mice developed more albuminuria than WT-STZ mice, we speculated whether these mice also developed more podocyte injury through glomerular endothelial cell-podocyte crosstalk. Electron microscopy of kidney sections revealed a significant increase in podocyte effacement in the KO-STZ mice compared to WT-STZ mice (Figure 9A, 9B). In addition, podocyte number was estimated by using a known podocyte marker, *Wilms-tumor 1 (Wt1). Wt1* mRNA expression levels or the number of Wt1 positive cells per glomerular cross section and per 1000 μm2 of glomerular areas was significantly reduced in both diabetic mice, with further reduction in KO-STZ mice as compared to WT-STZ mice (Figure 10A-D). The expression of podocyte-specific genes (nephrin, synaptopodin, podocin, and podocalyxin) was also reduced in KO-STZ mice compared to those from WT-STZ mice as determined by real- time PCR analysis of isolated glomeruli. This was confirmed by immunofluorescence staining of kidney sections (Figure 11A-11D).

DISCUSSION

In the current study, we have demonstrated a critical role of KLF2 in early DN. KLF2 is regulated by both high glucose and insulin and has a protective role against endothelial cell injury in early DN through transcriptional regulation of several key endothelial cell markers. Endothelial-specific knockdown of *Klf2* resulted in more glomerular endothelial cell injury as well as podocyte injury with induction of diabetes, suggesting a potential crosstalk between these two cell types.

Since there is a relative dearth of effective preventive measures in attenuating the progression of this disease, it is critical to identify the early event in DN. Unfortunately the current understanding of the pathogenesis of early DN remains unclear. This current study reveals a protective mechanism mediated by Klf2 in early DN and we observe that the removal of this protective mechanism results in more severe diabetic kidney injury.

Identifying the protective pathway in early DN may help elucidate the mechanism that mediates the variable rate of progression to DN observed in diabetic patients.

Previous studies suggest a potential crosstalk from the podocyte to the endothelial cell. Podocyte-secreted VEGF has a protective effect on endothelial cells (39), while podocyte-secreted endothelin-1 damages the endothelial cells by activation of oxidative stress (11). Our studies suggest that a crosstalk from the glomerular endothelial cell to the podocyte could also occur in early DN. Our data suggest that glomerular endothelial cell injury could lead to podocyte injury and the reduction of the podocyte differentiation markers in KO-STZ mice is likely a result of reduction in podocyte number, rather than podocyte dedifferentiation. The mechanism mediating this crosstalk requires further studies. Interestingly, KO-STZ mice developed more glomerular hypertrophy but the mesangial area fraction was not different in diabetic mice with or without *Klf2* knockdown. The mechanism of this observation is unclear. We speculate that the injured glomerular endothelial cells in KO-STZ mice may promote more glomerular cell hypertrophy instead of stimulation of extracellular matrix synthesis at the early stage of DN in this kidney disease-resistant mouse background (C57BL/6).

KLF2 is regulated by shear stress and has a protective role against endothelial cell injury (20). However, the role of KLF2 in DN has yet to be characterized. We initially speculated that glomerular KLF2 expression would be high in early DN due to the shear stress induced by hyperfiltration. However, we observed that Klf2 expression was significantly reduced in diabetic rats, likely due to hyperglycemia-induced suppression. Furthermore, normalization of hyperglycemia in these rats by insulin treatment raised Klf2 expression to a level higher than that of non-diabetic rats. This is likely due to the stimulation of Klf2 expression by insulin treatment based on our *in vitro* data. It would be interesting to determine whether hyperfiltration regulates Klf2 expression through induction of shear stress. However, our studies were not designed to address this question because normalization of hyperglycemia by insulin treatment also corrects hyperfiltration. We found that a more dramatic reduction of KLF2 expression was observed in human diabetic kidney. This is likely because diabetic patients have more advanced kidney disease while STZ-mice develop only early and mild DN. Also, it is possible that diabetic patients with low KLF2 expression develop more severe DN.

The mechanism by which KLF2 attenuates endothelial cell injury in the setting of diabetes needs to be studied. AMP kinase (AMPK) has been shown to mediate flow-induced KLF2 expression in endothelial cells (40). KLF2 facilitates the activation of the antioxidant transcription factor Nuclear Factor, Erythroid 2-like 2 (Nrf2) in endothelial cells (41). However, KLF2 expression is suppressed by oxidative stress through the redox enzyme p66shc (42). Interestingly, KLF2, in turn, inhibits p66shc expression through activation of APC (43). In addition, Nuclear Factor Kappa B (NF-KB) negatively regulates KLF2 expression (44), while KLF2 has anti-inflammatory effects through inhibition of NF-KB activation (45). These studies suggest a critical role of KLF2 in the regulation of oxidative stress and inflammation through these feedback mechanisms. Therefore, targeting the induction of KLF2 may attenuate DN through the activation of anti-oxidative stress and anti-inflammatory pathways.

KLF2 has been described to regulate many target genes involved in vascular endothelial cell development, differentiation, and function (20). Here, we determined that KLF2 regulates several key molecular markers of endothelial cells, including eNOS. Reduced eNOS expression is known to contribute to the pathogenesis of DN (5). Interestingly, eNOS was significantly lower in KO-STZ than WT-STZ mice while no difference was observed between non-diabetic WT and KO mice. In non-diabetic kidney, KLF2 may not have significant role in regulation of eNOS expression. However, in the diabetic kidney, eNOS expression, which is likely suppressed by high glucose and other factors, may require KLF2 to maintain its expression as a compensatory mechanism. In addition, KLF2 is a key regulator of thrombotic function (20). Knockdown of KLF2 reduces thrombomodulin expression (24) and the reduction of thrombomodulin is associated with the progression of DN (8). KLF2 also inhibits protease activated receptor-1 (PAR-1) expression and thrombin-mediated endothelial activation (46), and PAR-1 is increased in the diabetic kidney (8) and may mediate endothelial cell apoptosis in DN (47). The inactivation of Ang-1-Tie2 system is associated with increased permeability and leakage of plasma albumin in DN (48). The reduction of glomerular ZO-1 may also be responsible for the increased paracellular permeability and albuminuria observed in DN (49). Our data suggest that KLF2 up-regulates Ang1- Tie2 system and the expression of ZO-1, contributing to a potential mechanism by which KLF2 reduces albuminuria in mice with DN. Interestingly, we also observed a significant reduction of glycocalyx in non-diabetic KO mice while other endothelial cell markers did not change. The mechanism of this observation remains to be determined. Since these endothelial injury markers are regulated by multiple factors via different mechanisms, glycocalyx might be regulated by KLF2 via ann alternate mechanism as compared to these other markers.

Since glomerular endothelial cell-specific *Cre* mice are not available, we used a global endothelial cell-specific heterozygous *Klf2* knockout mouse, which had reduced Klf2 expression in all vascular endothelial cells. Consequently, the systemic effect of circulating factors released from non-glomerular endothelial cells injury cannot be neglected. The potential effects on endothelial injury resulting in elevated blood pressure were likely not the cause of the observed glomerular injury, since there were no significant differences in blood pressure between all four groups of mice. Homozygous mice were unable to be generated because these mice are embryonically lethal due to intra-embryonic and intra-amniotic hemorrhage (50).

In conclusion, our data suggest a potential role of KLF2 in diabetes-induced glomerular endothelial cell injury at the early stage of DN. Our findings also highlight a potential crosstalk from the glomerular endothelial cell to podocyte. Understanding the disease mechanisms in early DN may help shed light on novel preventive strategies against the development of this disease.

EXPERIMENTAL PROCEDURES

Experiments for STZ-rats

Male Sprague-Dawley (SD, 8 weeks old) rats were obtained from Jackson Research Laboratories (Bar Harbor, ME). Care, use, and treatment of all animals in this study were

approved by the Animal Care Committee at Icahn School of Medicine at Mount Sinai. Diabetes was induced in SD rats (8 weeks of age) by an intraperitoneal injection of streptozotocin (STZ) (60mg/kg in 10mmol/L of citrate buffer, pH 4.5) (Sigma, St. Louis, MO) after an overnight fast. Control rats received an injection of citrate buffer. Blood glucose levels were measured at 48 hours after the injection and monitored every 3 days thereafter. Only the animals with blood glucose concentrations >16.7mmol/l were considered diabetic. A group of diabetic rats received Neutral Insulin (16U/kg; Novo Nordisk, Copenhagen, Denmark) via subcutaneous injection twice a day from 6 to 12 weeks of diabetes for hyperglycemic control. Non-fasting glucose was monitored before the insulin injection. The kidney was removed when the mice were sacrificed for glomerular isolation and histology. 12-hour-urine samples were collected on the day before euthanasia by housing the animals in metabolic cages to determine the urine albumin excretion rate (Houston, TX).

Cell culture

Human umbilical venous cells (HUVECs) and human glomerular microvascular endothelial cells were cultured according to the manufacture instructions. Cells were serum starved in 1% serum containing medium for 12 hours followed by treatment with the medium containing either normal glucose (5mM) ± 25mM mannitol or high glucose (30mM) or insulin (100ng/ml) with or without high glucose for the indicated time intervals.

Western Blot

Cells were homogenized in lysis buffer containing protease inhibitor cocktail. Equal amounts of protein samples were electrophoretically separated on SDS polyacrylamide gel, transferred to PVDF membranes (Millipore) and probed with primary antibodies. Membranes were then washed with PBST and incubated with a secondary antibody (horseradish peroxidase conjugated antibodies to mouse IgG or to rabbit IgG). Blots were developed with the enhanced chemiluminescence system. Densitometry analysis for quantification was performed as described previously (51).

Generation of Conditional Klf2 Mice

SV/129 ES cells heterozygous for the *Klf2* conditional allele were generated by using standard gene-targeting techniques. $Klf2^{fl/+}$ mice were generated by deletion of exons 2 and 3 and provided by Dr. Mukesh Jain, a collaborator of this study. $KLF2^{fl/+}$ mice were viable, fertile, and born in the Mendelian ratios as expected in C57BL/6 background. *VEC-Cre* transgenic animals were purchased from Jackson Research Laboratories (Bar Harbor, ME). Endothelial cell specific heterozygous *Klf2* knockout mice (KO) were generated as described in the result section.

Diabetes model

All mice used in this study were on a congenic C57BL/6 background. At 8 weeks of age, male WT and KO mice were injected for 5 consecutive days with either STZ (50μg/g) (Sigma-Aldrich, St Louis, MO) per day intraperitoneally or sodium-citrate vehicle. Fasting blood glucose levels were monitored weekly by using a glucometer. All mice were housed

and cared for in the Animal Care Facility at out Institution with free access to food and water. All protocols were approved by the Animal Care Committee at Icahn School of Medicine at Mount Sinai.

Measurement of Urine Albumin and Creatinine

Urine albumin was quantified by ELISA using a kit from Bethyl Laboratories, Inc. (Houston, TX). Urine creatinine levels were measured in the same samples using QuantiChrom™ creatinine assay kit (DICT-500) (BioAssay Systems) according to the manufacturer's instruction. The urine albumin excretion rate was expressed as the ratio of albumin to creatinine.

Blood Pressure Monitoring

Blood pressure was measured using the CODA programmable non-invasive tail-cuff sphygmomanometer (Kent Scientific, Torrington, CT) on conscious mice as described (52). Mice were initially subjected to acclimation period of 5 cycles prior to blood pressure assessment. Subsequently, systolic blood pressure (SBP) was measured in each mouse for 60 continuous cycles and an average of SBP was quantified as previously described (52).

Kidney histology

Kidneys were removed and fixed with 4% paraformaldehyde for 48 hours at 4 °C. The 4Om sections were cut from paraffin-embedded kidney tissues. Sections were stained with periodic acid–Schiff for histology analysis. Assessment of the mesangial and glomerular cross-sectional areas was performed by pixel counts on a minimum of 10 glomeruli per section in a blinded fashion, under 400× magnification (Zeiss AX10 microscope, Carl Zeiss Canada Ltd, Toronto, ON, Canada).

Electron Microscopy

Tissues were fixed in 2.5% glutaraldehyde with 0.1M sodium cacodylate (pH 7.4) for 72 hr at 40°C. Samples were further incubated with 2% osmium tetroxide and 0.1M sodium cacodylate (pH 7.4) for 1 hr at 40°C. Ultrathin sections were stained with lead citrate and uranyl acetate and were viewed on a Hitachi H7650 microscope. Briefly, negatives were digitized, and images with a final magnitude of approximately X10,000 were obtained. ImageJ 1.26t software (National Institutes of Health, rsb.info.nih.gov) was used to measure the length of the peripheral GBM, and the number of slit pores overlying this GBM length was counted. The arithmetic mean of the foot process width (W_{FP}) was calculated as shown below:

$$W_{FP} = \frac{\pi}{4} \times \frac{\Sigma GBM \quad LENGTH}{\Sigma silts}$$

where Σslits indicates the total number of slits counted; ΣGBM LENGTH indicates the total GBM length measured in one glomerulus, and π/4 is the correction factor for the random orientation by which the foot processes were sectioned (53).

Isolation of Glomeruli from Mice for RNA Extraction

Mouse glomeruli were isolated as described (54). Briefly, animals were perfused with Hanks' buffered salt solution containing 2.5mg/ml iron oxide and 1% bovine serum albumin. At the end of perfusion, kidneys were removed, decapsulated, minced into 1mm^3 pieces, and digested in Hanks' buffered salt solution containing 1mg/ml collagenase A and 100units/ml deoxyribonuclease I. Digested tissue was then passed through a 100μm cell strainer and collected by centrifugation. The pellet was resuspended in 2 ml of Hanks' buffered salt solution, and glomeruli were collected using a magnet. The purity of glomerular was verified under microscopy. Total RNA was isolated from kidney glomeruli of mice using TRIzol (Invitrogen).

Isolation of Kidney Endothelial cells

After isolation of glomeruli, endothelial cells were isolated as described previously (55). In brief, isolated glomeruli were initially digested with collagenase/dispase (C/D) solution and dispersed mechanically into single-cell suspension. Mouse kidney endothelial cells (MKECs) were purified from cell suspension using positive selection with anti-PECAM-1 antibody (BD Pharmingen) conjugated to DynabeadsSheep anti-Rat IgG (Invitrogen) using a Magnetic Particle Concentrator (MPC). Purified cells were cultured on gelatin-coated tissue culture dishes until they became confluent. Next, endothelial cells were further purified using Dynabeads coupled to anti- ICAM-2 antibody and cultured on collagen I-coated dishes. Isolated endothelial cells were characterized by immunostaining and real-time PCR analysis for endothelial markers was performed.

Real-time PCR

Total RNA was extracted by using TRIzol (Invitrogen). First strand cDNA was prepared from total RNA (2.0 μg) using the Superscript ™ III first strand synthesis kit (Invitrogen), and cDNA (1 μl) was amplified in triplicate using SYBR GreenER qPCR Supermix on an ABI PRISM 7900HT (Applied Biosystems, Foster City, CA). The primer sequences are listed in Table 1. Light Cycler analysis software was used to determine crossing points using the second derivative method. Data were normalized to housekeeping genes (GAPDH) and presented as fold increase compared with RNA isolated from WT animals using the 2-ΔΔ^{CT} method.

Immunofluorescence

Kidney sections from these mice were prepared in an identical fashion. Immunostaining was performed using rabbit anti-synaptopodin (Fitzgerald), rabbit anti-nephrin (a gift from Dr. Larry Holzman), and mouse anti-WT1 antibodies (Santa Cruz Biotechnology). After washing, sections were incubated with a fluorophore-linked secondary antibody (Alexa Fluor 488 anti-rabbit IgG and Alexa Fluor 568 anti-mouse IgG from Invitrogen). After staining, slides were mounted in Aqua Poly/Mount (Polysciences Inc.) and photographed under an AxioVision IIe microscope with a digital camera.

Immunohistochemistry

Archival human biopsy specimens of healthy donor nephrectomies and diabetic nephropathy were collected at Icahn School of Medicine at Mount Sinai under a protocol approved by the Institutional Review Board. Specimens were initially baked for 20 minutes in 55–60 °C oven and then processed as described previously below. Briefly formalin-fixed and paraffin-embedded sections were deparaffinized, and endogenous peroxidase was inactivated with H_2O_2. Sections were then blocked in 2% goat serum in phosphate-buffered saline (PBS) for 1 hour at room temperature and then incubated with a rabbit anti-KLF2 antibody (1:1000, GenScript) at 4°C overnight. The next day, sections were washed three times with PBS and then incubated with secondary antibody for 30 minutes. Positive staining was revealed by peroxidase-labeled streptavidin and diaminobenzidine substrate. The control included a section stained with only secondary antibody.

Quantification of Immunostaining

After sections were stained with anti-KLF2 antibody, negatives were digitized, and images with a final magnitude of approximately X400 were obtained. ImageJ 1.26t software was used to measure the level of immunostaining in the glomeruli. First, the images were converted to 8-bit grayscale. Next, the glomerular region was selected for measurement of area and integrated density. Next, the background intensity was measured by selecting three distinct areas in the background with no staining. The corrected optical density (COD) was determined as shown below:

$$COD=ID-(A\times MGV)$$

where ID is the integrated density of the selected glomerular region, A is the area of the selected glomerular region, and MGV is the mean gray value of the background readings) (56).

Statistical Analysis

Data were expressed as mean ± SEM. The unpaired t test was used to analyze data between two groups. The analysis of variance followed by Bonferroni correction was used when more than two groups were present. All experiments were repeated at least three times, and representative experiments are shown. Statistical significance will be considered when $p<0.05$.

Supplementary Material

Refer to Web version on PubMed Central for supplementary material.

Acknowledgment

JCH is supported by VA Merit Award, NIH 1R01DK078897, NIH 1R01DK088541, NIH P01-DK-56492, and Chinese 973 fund 2012CB517601; Dr. John He is the guarantor of this work and, as such, had full access to all the data in the study and takes responsibility for the integrity of the data and the accuracy of the data analysis.

References

1. Collins AJ, Foley RN, Chavers B, Gilbertson D, Herzog C, Ishani A, Johansen K, Kasiske BL, Kutner N, Liu J, et al. US Renal Data System 2013 Annual Data Report. Am J Kidney Dis. 2014; 63:A7. [PubMed: 24360288]
2. Premaratne E, Macisaac RJ, Tsalamandris C, Panagiotopoulos S, Smith T, Jerums G. Renal hyperfiltration in type 2 diabetes: effect of age-related decline in glomerular filtration rate. Diabetologia. 2005; 48:2486–2493. [PubMed: 16261309]
3. Wolf G, Chen S, Ziyadeh FN. From the periphery of the glomerular capillary wall toward the center of disease: podocyte injury comes of age in diabetic nephropathy. Diabetes. 2005; 54:1626–1634. [PubMed: 15919782]
4. Dei Cas A, Gnudi L. VEGF and angiopoietins in diabetic glomerulopathy: how far for a new treatment? Metabolism. 2012; 61:1666–1673. [PubMed: 22554833]
5. Yuen DA, Stead BE, Zhang YL, White KE, Kabir MG, Thai K, Advani SL, Connelly KA, Takano T, Zhu L, et al. eNOS Deficiency Predisposes Podocytes to Injury in Diabetes. Journal of the American Society of Nephrology. 2012; 23:1810–1823. [PubMed: 22997257]
6. Zhao HJ, Wang S, Cheng H, Zhang MZ, Takahashi T, Fogo AB, Breyer MD, Harris RC. Endothelial nitric oxide synthase deficiency produces accelerated nephropathy in diabetic mice. J Am Soc Nephrol. 2006; 17:2664–2669. [PubMed: 16971655]
7. Nakagawa T. Uncoupling of the VEGF-endothelial nitric oxide axis in diabetic nephropathy: an explanation for the paradoxical effects of VEGF in renal disease. Am J Physiol Renal Physiol. 2007; 292:F1665–1672. [PubMed: 17545302]
8. Isermann B, Vinnikov IA, Madhusudhan T, Herzog S, Kashif M, Blautzik J, Corat MA, Zeier M, Blessing E, Oh J, et al. Activated protein C protects against diabetic nephropathy by inhibiting endothelial and podocyte apoptosis. Nat Med. 2007; 13:1349–1358. [PubMed: 17982464]
9. Haraldsson B, Nystrom J. The glomerular endothelium: new insights on function and structure. Curr Opin Nephrol Hypertens. 2012; 21:258–263. [PubMed: 22388551]
10. Salmon AH, Satchell SC. Endothelial glycocalyx dysfunction in disease: albuminuria and increased microvascular permeability. J Pathol. 2012; 226:562–574. [PubMed: 22102407]
11. Daehn I, Casalena G, Zhang T, Shi S, Fenninger F, Barasch N, Yu L, D'Agati V, Schlondorff D, Kriz W, et al. Endothelial mitochondrial oxidative stress determines podocyte depletion in segmental glomerulosclerosis. J Clin Invest. 2014; 124:1608–1621. [PubMed: 24590287]
12. Feinberg MW, Lin Z, Fisch S, Jain MK. An emerging role for Kruppel-like factors in vascular biology. Trends Cardiovasc Med. 2004; 14:241–246. [PubMed: 15451516]
13. Pearson R, Fleetwood J, Eaton S, Crossley M, Bao S. Kruppel-like transcription factors: a functional family. Int J Biochem Cell Biol. 2008; 40:1996–2001. [PubMed: 17904406]
14. Kuo CT, Veselits ML, Leiden JM. LKLF: A transcriptional regulator of single-positive T cell quiescence and survival. Science. 1997; 277:1986–1990. [PubMed: 9302292]
15. Carlson CM, Endrizzi BT, Wu J, Ding X, Weinreich MA, Walsh ER, Wani MA, Lingrel JB, Hogquist KA, Jameson SC. Kruppel-like factor 2 regulates thymocyte and T-cell migration. Nature. 2006; 442:299–302. [PubMed: 16855590]
16. Das H, Kumar A, Lin Z, Patino WD, Hwang PM, Feinberg MW, Majumder PK, Jain MK. Kruppel-like factor 2 (KLF2) regulates proinflammatory activation of monocytes. Proc Natl Acad Sci U S A. 2006; 103:6653–6658. [PubMed: 16617118]
17. Weinreich MA, Takada K, Skon C, Reiner SL, Jameson SC, Hogquist KA. KLF2 transcription-factor deficiency in T cells results in unrestrained cytokine production and upregulation of bystander chemokine receptors. Immunity. 2009; 31:122–130. [PubMed: 19592277]
18. Lee JS, Yu Q, Shin JT, Sebzda E, Bertozzi C, Chen M, Mericko P, Stadtfeld M, Zhou D, Cheng L, et al. Klf2 is an essential regulator of vascular hemodynamic forces in vivo. Dev Cell. 2006; 11:845–857. [PubMed: 17141159]
19. Parmar KM, Larman HB, Dai G, Zhang Y, Wang ET, Moorthy SN, Kratz JR, Lin Z, Jain MK, Gimbrone MA Jr. et al. Integration of flow-dependent endothelial phenotypes by Kruppel-like factor 2. J Clin Invest. 2006; 116:49–58. [PubMed: 16341264]

20. Atkins GB, Jain MK. Role of Kruppel-like transcription factors in endothelial biology. Circ Res. 2007; 100:1686–1695. [PubMed: 17585076]
21. Lin ZY, Natesan V, Shi H, Dong F, Kawanami D, Mahabeleshwar GH, Atkins GB, Nayak L, Cui YJ, Finigan JH, et al. Kruppel-Like Factor 2 Regulates Endothelial Barrier Function. Arteriosclerosis Thrombosis and Vascular Biology. 2010; 30:1952–U1181.
22. Chiplunkar AR, Curtis BC, Eades GL, Kane MS, Fox SJ, Haar JL, Lloyd JA. The Kruppel-like factor 2 and Kruppel-like factor 4 genes interact to maintain endothelial integrity in mouse embryonic vasculogenesis. BMC Dev Biol. 2013; 13:40. [PubMed: 24261709]
23. Bhattacharya R, Senbanerjee S, Lin Z, Mir S, Hamik A, Wang P, Mukherjee P, Mukhopadhyay D, Jain MK. Inhibition of vascular permeability factor/vascular endothelial growth factor-mediated angiogenesis by the Kruppel-like factor KLF2. J Biol Chem. 2005; 280:28848–28851. [PubMed: 15980434]
24. Lin Z, Kumar A, SenBanerjee S, Staniszewski K, Parmar K, Vaughan DE, Gimbrone MA Jr. Balasubramanian V, Garcia-Cardena G, Jain MK. Kruppel-like factor 2 (KLF2) regulates endothelial thrombotic function. Circ Res. 2005; 96:e48–57. [PubMed: 15718498]
25. SenBanerjee S, Lin Z, Atkins GB, Greif DM, Rao RM, Kumar A, Feinberg MW, Chen Z, Simon DI, Luscinskas FW, et al. KLF2 Is a novel transcriptional regulator of endothelial proinflammatory activation. J Exp Med. 2004; 199:1305–1315. [PubMed: 15136591]
26. Agustian PA, Bockmeyer CL, Modde F, Wittig J, Heinemann FM, Brundiers S, Dammrich ME, Schwarz A, Birschmann I, Suwelack B, et al. Glomerular mRNA expression of prothrombotic and antithrombotic factors in renal transplants with thrombotic microangiopathy. Transplantation. 2013; 95:1242–1248. [PubMed: 23635876]
27. Slater SC, Ramnath RD, Uttridge K, Saleem MA, Cahill PA, Mathieson PW, Welsh GI, Satchell SC. Chronic exposure to laminar shear stress induces Kruppel-like factor 2 in glomerular endothelial cells and modulates interactions with co-cultured podocytes. Int J Biochem Cell Biol. 2012; 44:1482–1490. [PubMed: 22683691]
28. Lee HY, Youn SW, Oh BH, Kim HS. Kruppel-like factor 2 suppression by high glucose as a possible mechanism of diabetic vasculopathy. Korean Circ J. 2012; 42:239–245. [PubMed: 22563336]
29. Azeloglu EU, Hardy SV, Eungdamrong NJ, Chen Y, Jayaraman G, Chuang PY, Fang W, Xiong H, Neves SR, Jain MR, et al. Interconnected network motifs control podocyte morphology and kidney function. Sci Signal. 2014; 7:ra12. [PubMed: 24497609]
30. Hodgin JB, Nair V, Zhang H, Randolph A, Harris RC, Nelson RG, Weil EJ, Cavalcoli JD, Patel JM, Brosius FC 3rd, et al. Identification of cross-species shared transcriptional networks of diabetic nephropathy in human and mouse glomeruli. Diabetes. 2013; 62:299–308. [PubMed: 23139354]
31. Mallipattu SK, Liu R, Zheng F, Narla G, Ma'ayan A, Dikman S, Jain MK, Saleem M, D'Agati V, Klotman P, et al. Kruppel-like factor 15 (KLF15) is a key regulator of podocyte differentiation. J Biol Chem. 2012; 287:19122–19135. [PubMed: 22493483]
32. Dekker RJ, Boon RA, Rondaij MG, Kragt A, Volger OL, Elderkamp YW, Meijers JCM, Voorberg J, Pannekoek H, Horrevoets AJG. KLF2 provokes a gene expression pattern that establishes functional quiescent differentiation of the endothelium. Blood. 2006; 107:4354–4363. [PubMed: 16455954]
33. Satchell SC, Tooke JE. What is the mechanism of microalbuminuria in diabetes: a role for the glomerular endothelium? Diabetologia. 2008; 51:714–725. [PubMed: 18347777]
34. Wingender E, Chen X, Hehl R, Karas H, Liebich I, Matys V, Meinhardt T, Pruss M, Reuter I, Schacherer F. TRANSFAC: an integrated system for gene expression regulation. Nucleic Acids Res. 2000; 28:316–319. [PubMed: 10592259]
35. Wasserman WW, Sandelin A. Applied bioinformatics for the identification of regulatory elements. Nat Rev Genet. 2004; 5:276–287. [PubMed: 15131651]
36. Cartharius K, Frech K, Grote K, Klocke B, Haltmeier M, Klingenhoff A, Frisch M, Bayerlein M, Werner T. MatInspector and beyond: promoter analysis based on transcription factor binding sites. Bioinformatics. 2005; 21:2933–2942. [PubMed: 15860560]

37. Dellamea BS, Leitao CB, Friedman R, Canani LH. Nitric oxide system and diabetic nephropathy. Diabetol Metab Syndr. 2014; 6:17. [PubMed: 24520999]

38. Cheng H, Wang H, Fan X, Paueksakon P, Harris RC. Improvement of endothelial nitric oxide synthase activity retards the progression of diabetic nephropathy in db/db mice. Kidney Int. 2012; 82:1176–1183. [PubMed: 22785174]

39. Sivaskandarajah GA, Jeansson M, Maezawa Y, Eremina V, Baelde HJ, Quaggin SE. Vegfa protects the glomerular microvasculature in diabetes. Diabetes. 2012; 61:2958–2966. [PubMed: 23093658]

40. Young A, Wu W, Sun W, Benjamin Larman H, Wang N, Li YS, Shyy JY, Chien S, Garcia-Cardena G. Flow activation of AMP-activated protein kinase in vascular endothelium leads to Kruppel-like factor 2 expression. Arterioscler Thromb Vasc Biol. 2009; 29:1902–1908. [PubMed: 19696400]

41. Fledderus JO, Boon RA, Volger OL, Hurttila H, Yla-Herttuala S, Pannekoek H, Levonen AL, Horrevoets AJ. KLF2 primes the antioxidant transcription factor Nrf2 for activation in endothelial cells. Arterioscler Thromb Vasc Biol. 2008; 28:1339–1346. [PubMed: 18467642]

42. Kumar A, Hoffman TA, Dericco J, Naqvi A, Jain MK, Irani K. Transcriptional repression of Kruppel like factor-2 by the adaptor protein p66shc. FASEB J. 2009; 23:4344–4352. [PubMed: 19696221]

43. Bock F, Shahzad K, Wang H, Stoyanov S, Wolter J, Dong W, Pelicci PG, Kashif M, Ranjan S, Schmidt S, et al. Activated protein C ameliorates diabetic nephropathy by epigenetically inhibiting the redox enzyme p66Shc. Proc Natl Acad Sci U S A. 2013; 110:648–653. [PubMed: 23267072]

44. Zahlten J, Steinicke R, Opitz B, Eitel J, N'Guessan P D, Vinzing M, Witzenrath M, Schmeck B, Hammerschmidt S, Suttorp N, et al. TLR2- and nucleotide-binding oligomerization domain 2-dependent Kruppel-like factor 2 expression downregulates NF-kappa B-related gene expression. J Immunol. 2010; 185:597–604. [PubMed: 20525885]

45. Nayak L, Goduni L, Takami Y, Sharma N, Kapil P, Jain MK, Mahabeleshwar GH. Kruppel-like factor 2 is a transcriptional regulator of chronic and acute inflammation. Am J Pathol. 2013; 182:1696–1704. [PubMed: 23499374]

46. Lin Z, Hamik A, Jain R, Kumar A, Jain MK. Kruppel-like factor 2 inhibits protease activated receptor-1 expression and thrombin-mediated endothelial activation. Arterioscler Thromb Vasc Biol. 2006; 26:1185–1189. [PubMed: 16514085]

47. Sakai T, Nambu T, Katoh M, Uehara S, Fukuroda T, Nishikibe M. Up-regulation of protease-activated receptor-1 in diabetic glomerulosclerosis. Biochem Biophys Res Commun. 2009; 384:173–179. [PubMed: 19401193]

48. London NR, Whitehead KJ, Li DY. Endogenous endothelial cell signaling systems maintain vascular stability. Angiogenesis. 2009; 12:149–158. [PubMed: 19172407]

49. Macconi D, Ghilardi M, Bonassi ME, Mohamed EI, Abbate M, Colombi F, Remuzzi G, Remuzzi A. Effect of angiotensin-converting enzyme inhibition on glomerular basement membrane permeability and distribution of zonula occludens-1 in MWF rats. Journal of the American Society of Nephrology. 2000; 11:477–489. [PubMed: 10703671]

50. Wani MA, Means RT Jr. Lingrel JB. Loss of LKLF function results in embryonic lethality in mice. Transgenic Res. 1998; 7:229–238. [PubMed: 9859212]

51. Gassmann M, Grenacher B, Rohde B, Vogel J. Quantifying Western blots: pitfalls of densitometry. Electrophoresis. 2009; 30:1845–1855. [PubMed: 19517440]

52. Kume S, Uzu T, Araki S, Sugimoto T, Isshiki K, Chin-Kanasaki M, Sakaguchi M, Kubota N, Terauchi Y, Kadowaki T, et al. Role of altered renal lipid metabolism in the development of renal injury induced by a high-fat diet. J Am Soc Nephrol. 2007; 18:2715–2723. [PubMed: 17855643]

53. Koop K, Eikmans M, Baelde HJ, Kawachi H, De Heer E, Paul LC, Bruijn JA. Expression of podocyte-associated molecules in acquired human kidney diseases. J Am Soc Nephrol. 2003; 14:2063–2071. [PubMed: 12874460]

54. Takemoto M, Asker N, Gerhardt H, Lundkvist A, Johansson BR, Saito Y, Betsholtz C. A new method for large scale isolation of kidney glomeruli from mice. Am J Pathol. 2002; 161:799–805. [PubMed: 12213707]

55. Sobczak M, Dargatz J, Chrzanowska-Wodnicka M. Isolation and culture of pulmonary endothelial cells from neonatal mice. J Vis Exp. 2010

56. Potapova TA, Sivakumar S, Flynn JN, Li R, Gorbsky GJ. Mitotic progression becomes irreversible in prometaphase and collapses when Wee1 and Cdc25 are inhibited. Molecular Biology of the Cell. 2011; 22:1191–1206. [PubMed: 21325631]

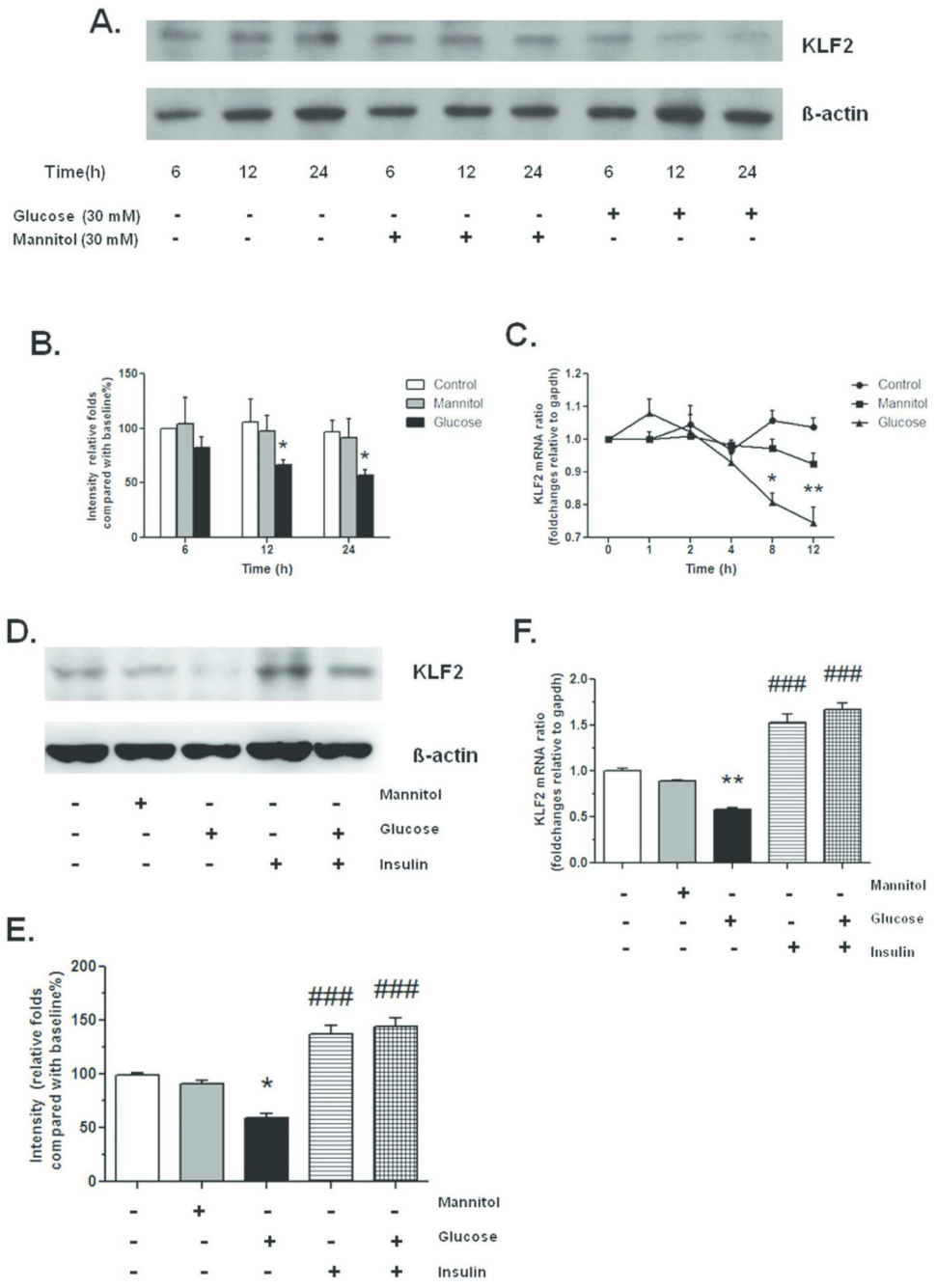

Figure 1. High glucose suppresses KLF2 expression in endothelial cells

HUVEC were incubated with high glucose (30mM) or normal glucose (5mM) ± mannitol (25mM) for 24 hours. Western blots were performed in these cells for KLF2. (A) Representative blots of three independent experiments are shown. (B) The densitometry analyses were performed for western blots. (C) *KLF2* mRNA expression was measured by real-time PCR. (D) Human glomerular microvascular endothelial cells were incubated with high glucose (30mM) or normal glucose (5mM) ± mannitol (25mM) with or without insulin (100ng/ml) for 24 hours. Representative blots of three independent experiments are shown. (E) The densitometry analyses were performed for western blots. (F) *KLF2* mRNA

expression was measured by real-time PCR *p<0.05, **p<0.01 compared to all other groups, ###p<0.001 compared to mannitol. The mean ± SEM of three independent experiments is shown (Control: 5mM glucose).

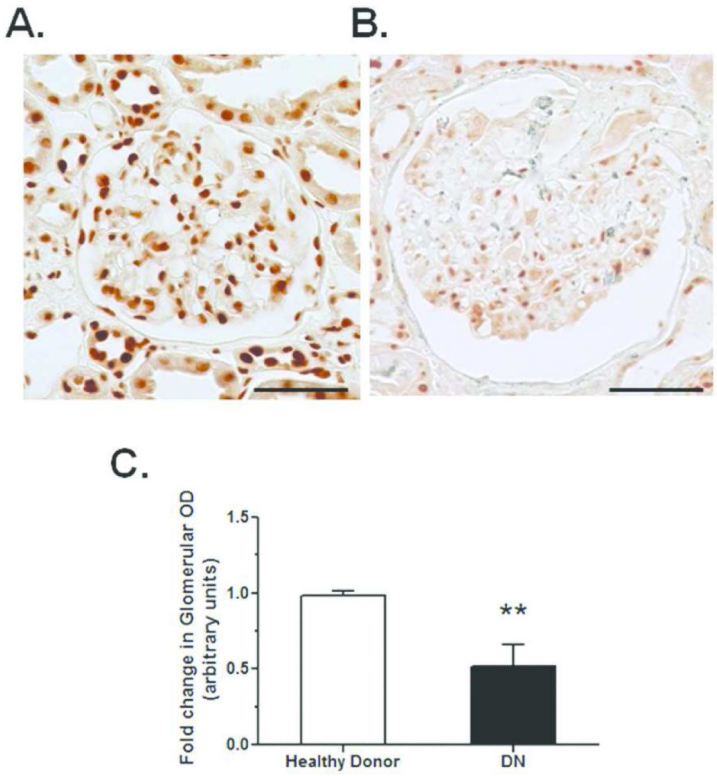

Figure 2. KLF2 expression is reduced in human diabetic nephropathy

Immunostaining for KLF2 was performed on healthy donor nephrectomy specimens (A) and kidney biopsies of patients with DN (B). The representative images of six subjects in each group are shown (original magnification × 400, scale bar: 50Om). (C*)* Glomerular area was selected, and optical density (*OD*) was measured and quantified as a relative fold change to healthy donor specimens (n = 6, **p<0.01).

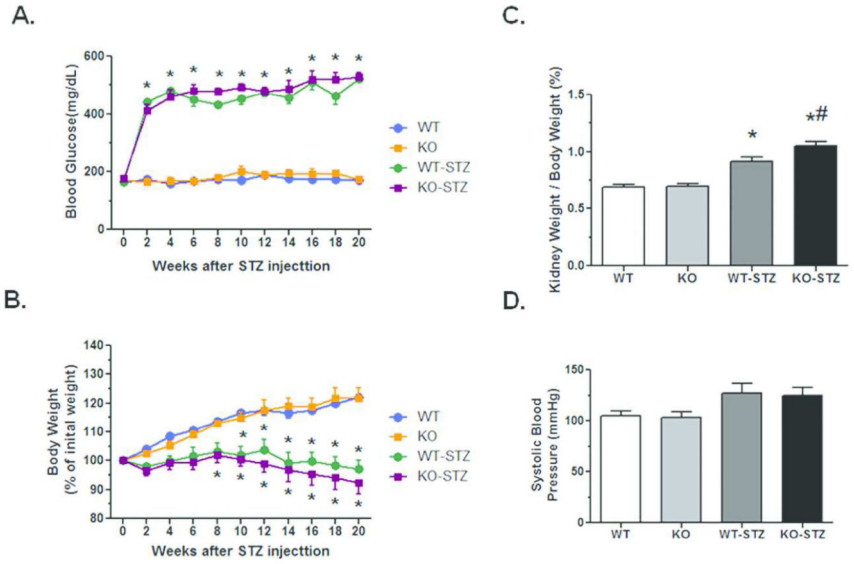

Figure 3. Blood glucose, body weight, kidney weight and systolic blood pressure measurements in WT and KO mice treated with and without STZ

(A) WT and KO mice treated with STZ (WT-STZ and KO-STZ) developed severe diabetes with significantly increased plasma glucose levels compared with vehicle- treated mice but no significant difference was found between the two STZ groups. (n=6, *p<0.001 compared to non-STZ mice). (B) KO mice had lower body weights than age- matched WT mice. However, both WT-STZ and KO-STZ mice experienced weight loss. (C) They developed renal hypertrophy with increased kidney weight to body weight ratio (n=6, *p<0.001 versus untreated mice, $^{\#}$p<0.05 compared to WT-STZ). (D) Systolic blood pressure was measured at 20 weeks after STZ injection by tail-cuff plethysmography.

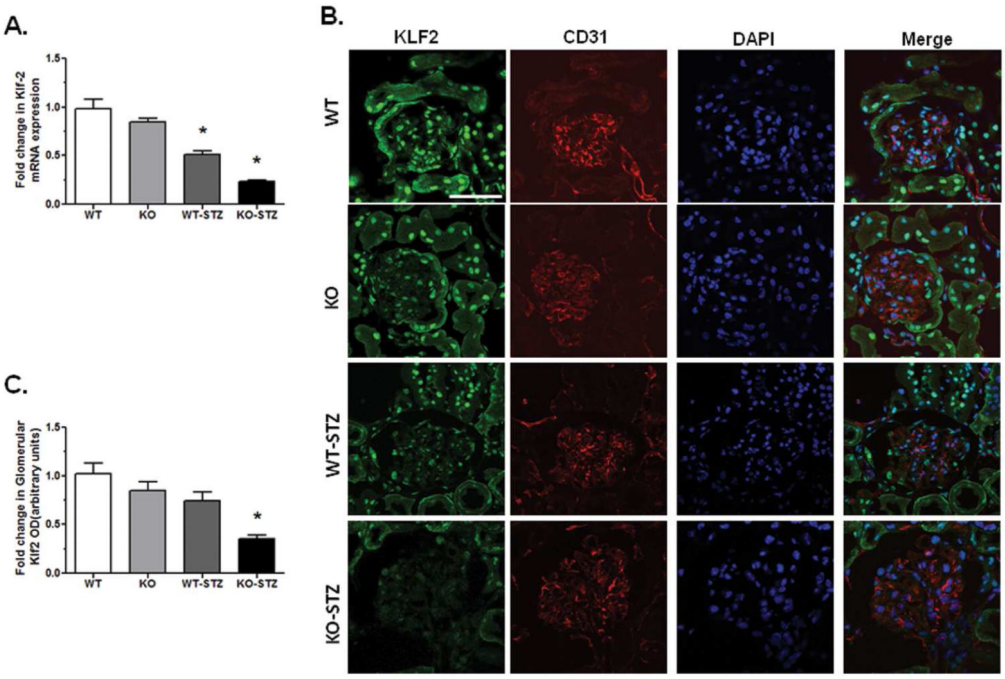

Figure 4. Klf2 expression is reduced in diabetic mice

(A) Klf2 mRNA expression in the glomeruli was compared between STZ-WT, STZ-KO, and non-STZ mice (n = 6, *p <0.05 compared to all other groups). (B) The representative pictures of immunofluorescence for Klf2 and co-staining with the endothelial protein PECAM-1 (CD31) and DAPI are shown (original magnification ×400, scale bar: 50μm). (C) Optical density (*OD*) was measured and quantified as a relative fold change to WT (*n* = 60 glomeruli per group of 6 mice; *p<0.05 compared to all other groups).

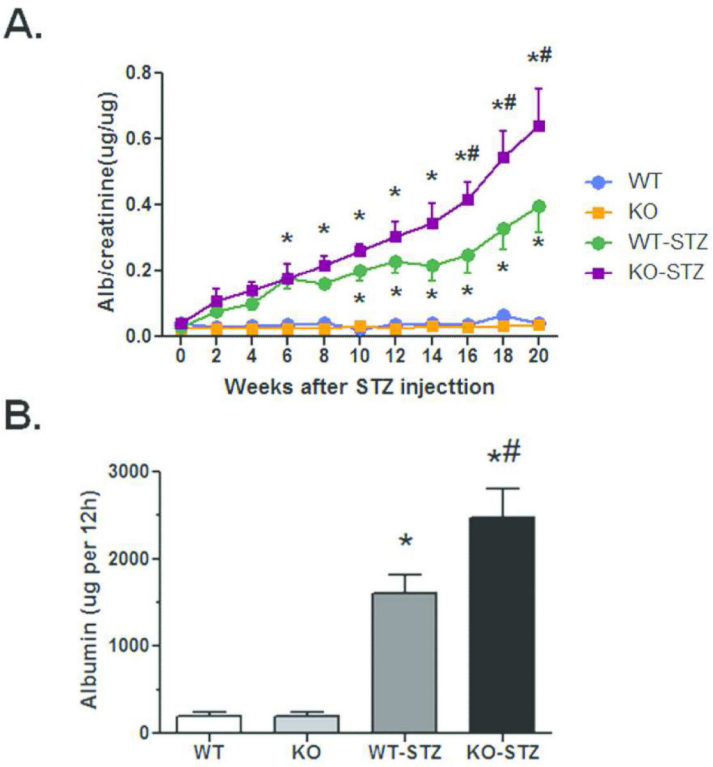

Figure 5. Urine albumin excretion rate is increase in KO-STZ mice

(A) Albuminuria (albuminuria/creatinine) was measured in WT-STZ and KO-STZ mice. (B) The 12-hour urinary albumin excretion rate was determined at 20 weeks after STZ injection (n = 6, *p<0.001 compared to WT and KO mice, #p<0.05 compared to WT-STZ).

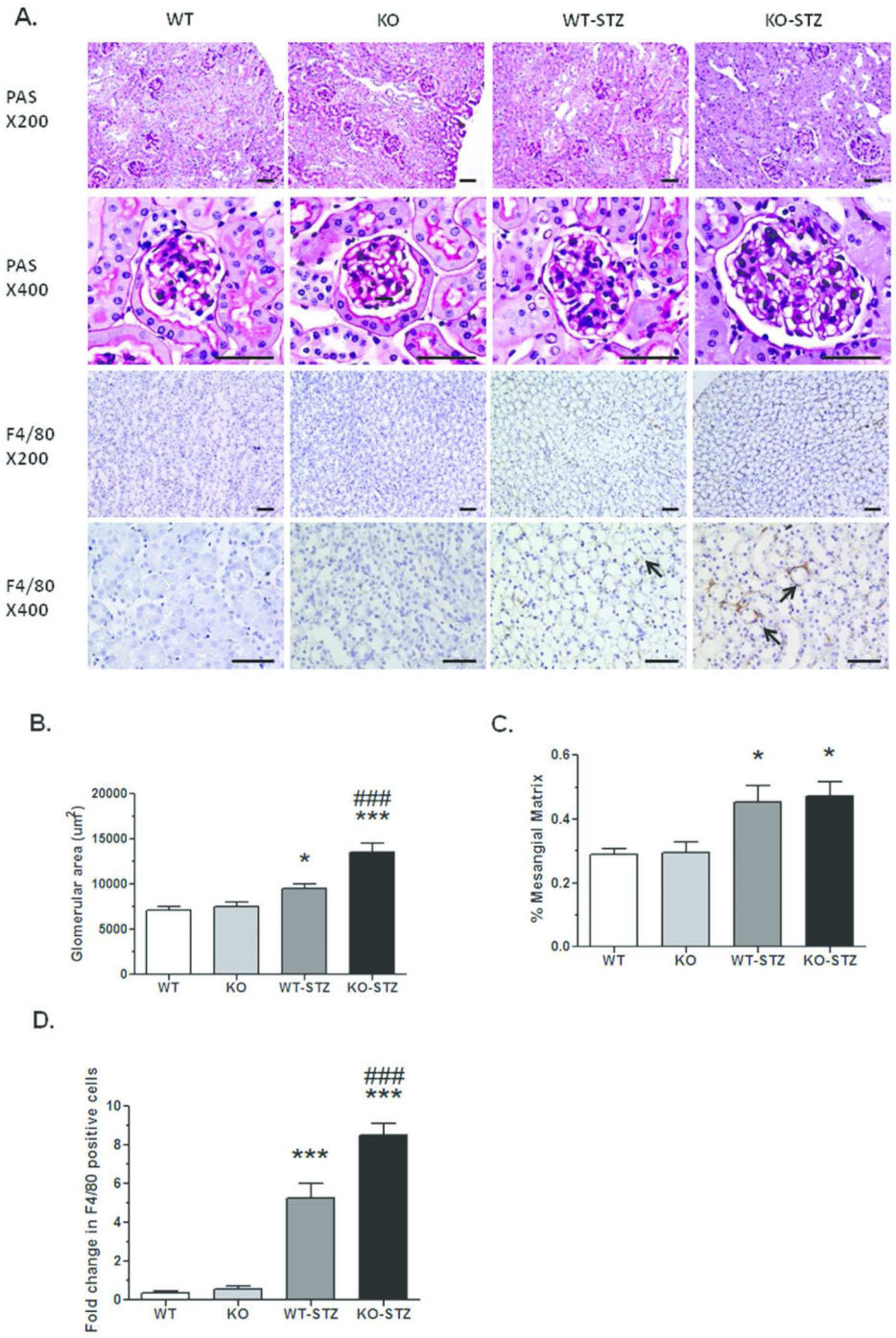

Figure 6. Effect of KLF2 knockdown on mesangial and glomerular area at 20 weeks after STZ injection

(A) Representative pictures of periodic acid–Schiff (PAS) and F4/80 in WT, KO, WT STZ, and KO-STZ mice at 20 weeks after STZ injection at both low and high powers. Glomerular hypertrophy and increased mesangial staining is shown in STZ groups as compared to non-STZ mice. (B) Glomerular area quantification is shown at 20 weeks after STZ injection. (C) The percentage of mesangial matrix area in the glomeruli at 20 weeks after STZ injection is

quantified in the diabetic mice and the non-diabetic mice. (D) Quantification of F4/80-positive cells between diabetic mice and non-diabetic mice. (60 glomeruli per group, n=6 mice, *P<0.05 vs non-STZ mice, ***P<0.001 vs non-STZ mice; ###P<0.001 vs WT-STZ; Original magnification x 200 and x 400, Scale bar: 50Oμm).

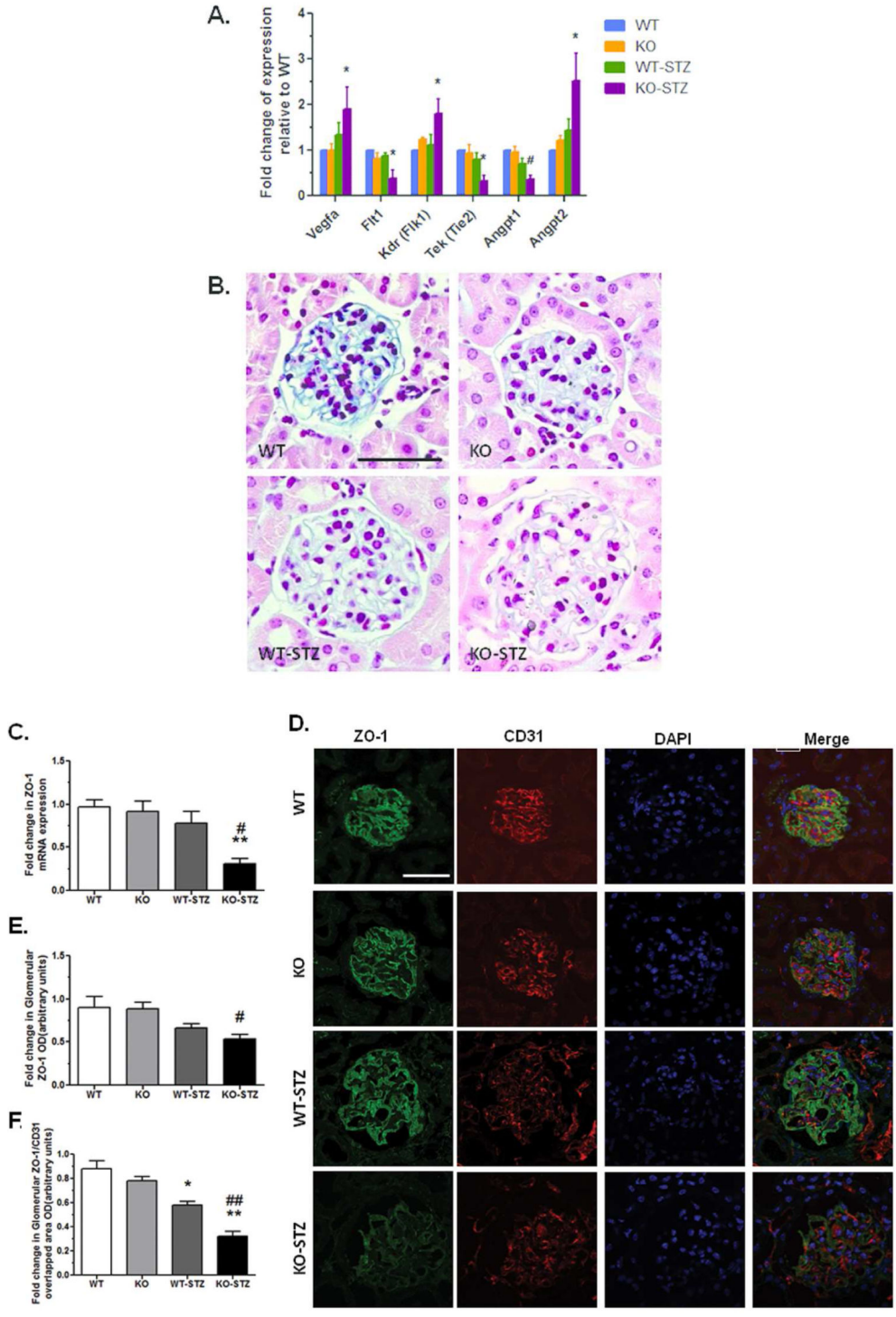

Figure 7. Knockdown of Klf2 causes more injury of glomerular endothelial cells in diabetic mice

(A) *Vegfa, Flt1, Kdr(Flk1), Tek(Tie2), Angpt1* and *Angpt2* mRNA levels were measured in the isolated glomeruli of mice from each group of mice (n=6, *p<0.05 compared to all other groups, #p<0.05 compared to WT and KO mice). (B) Representative pictures of staining for glycocalyx in WT, KO, WT-STZ, KO-STZ mice at 20 weeks after STZ injection is shown

(original magnification × 400, scale bar: 50μm). (C) mRNA levels of *ZO-1 (Tjp1)* were measured between each groups of mice using real-time PCR (n=6, *p<0.05 compared to all other groups). (D) The representative pictures of immunofluorescence for ZO-1 and CD31 are shown (Original magnification × 400, Scale bar, 50μm). (E) Optical density (*OD*) was measured and quantified for the areas with ZO-I positive staining in each glomerulus and was expressed as a relative fold change to WT mice (60 glomeruli per group; n=6, $^{\#}$p<0.05 compared to WT and KO mice). (F) Optical density (*OD*) was measured and quantified for the areas with both ZO-1 and CD31 positive staining in each glomerulus and was expressed as a relative fold change to WT mice (60 glomeruli per group; n=6, *p<0.05 vs WT mice, **p<0.01 vs KO mice; $^{\#}$p<0.05 vs WT-STZ, $^{\#\#}$p<0.01 vs WT-STZ).

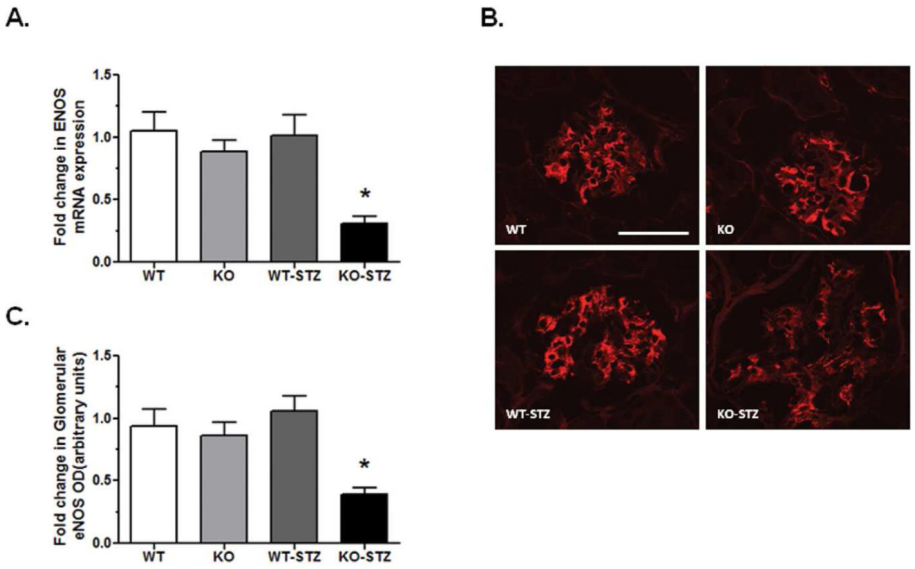

Figure 8. Effect of Klf2 Knockdown on eNOS expression

(A) mRNA levels of eNOS were compared between each group of mice. (n=6, *p<0.05 compared to all other group). (B) Immunofluorescence staining of eNOS is shown (original magnification ×400, scale bar: 50μm). (C) Optical density (*OD*) was measured and quantified as relative fold changes to WT mice (60 glomeruli per group; n=6, *p<0.05 compared to all other group).

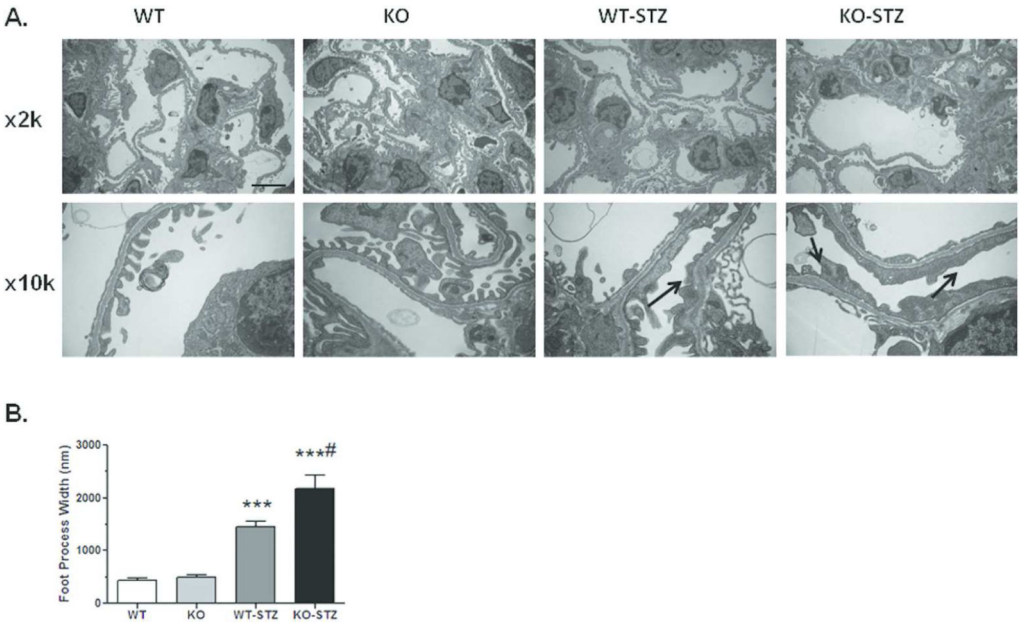

Figure 9. Podocyte foot process effacement is increased in KO-STZ mice

(A) Representative pictures of electronic microscopy from the WT, KO, WT-STZ, KO- STZ mice are shown with both low (2K) and high (10K) magnifications (scale bar: 5Om). (B) Quantification of foot process effacement is shown. (60 glomeruli per group; n=6, ***$p<0.001$ compared to WT and KO, $^{\#}P<0.05$ compared to WT-STZ).

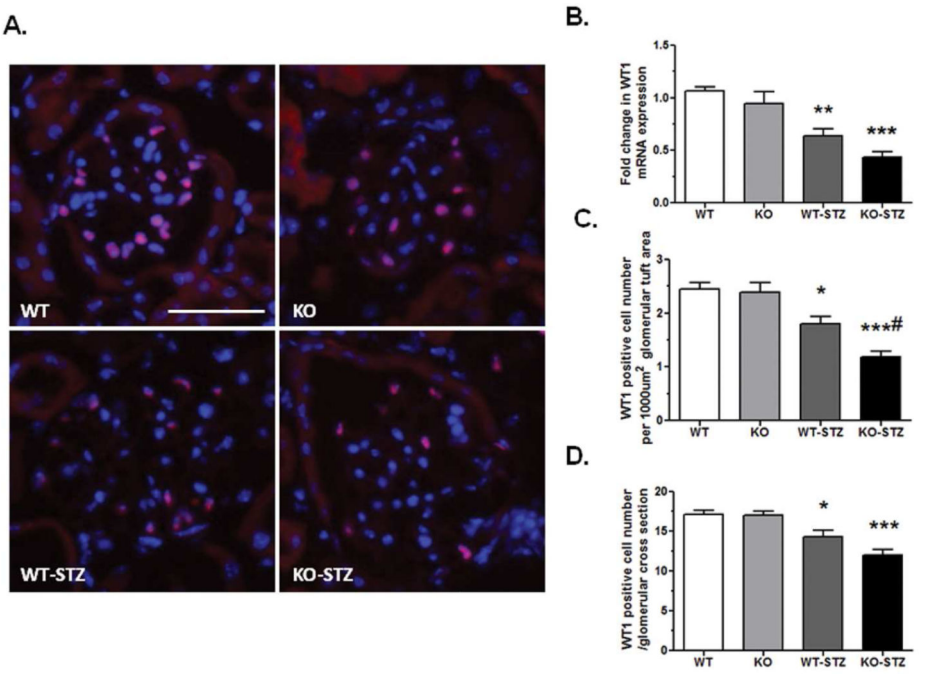

Figure 10. Glomerular podocyte number is reduced in KO-STZ mice

(A) The representative pictures of WT1 staining in glomeruli are shown (n=6, original magnification ×400, scale bar: 50μm). (B) mRNA levels of WT1 were measured using real-time PCR. (C) WT1 positive cell number/glomerular cross section and (D) WT1 positive cell number per 1000 μm^2 glomerular tuft area were quantified and expressed as relative fold changes to WT mice. (60 glomeruli per group; n=6, ***p<0.001 compared to WT and KO, **p <0.01 compared to WT and p<0.05 compared to KO, *p <0.05 compared to WT and KO, $^{\#}$p <0.05 compared to WT-STZ).

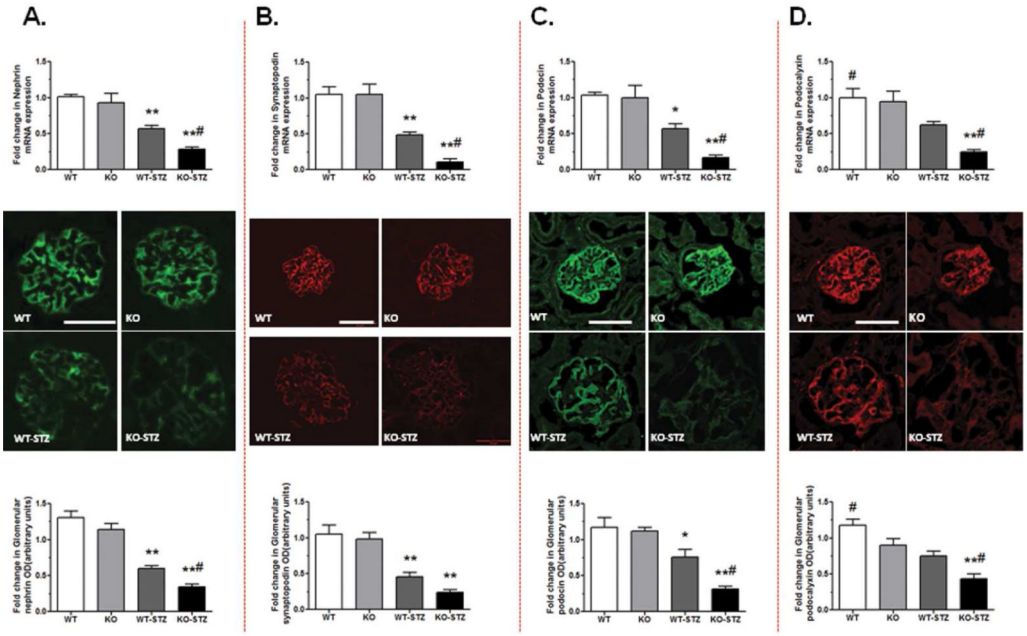

Figure 11. Expression of podocyte differentiation markers is reduced in KO-STZ mice

Top panel: mRNA levels of nephrin (*A*), synaptopodin (*B*), podocin (*C*), and podocalyxin (D) were compared between all four groups of mice. Middle panel: This was confirmed by immunofluorescence. The representative pictures of three mice in each group are shown. Bottom panel: The glomerular area was selected, and optical density (*OD*) was quantified as relative fold change to WT mice. (60 glomeruli per group; n=6, **p<0.01 compared to WT and KO, *p <0.05 compared to WT and KO, $^{\#}$p <0.05 compared to WT- STZ, original magnification ×400, scale bar: 50μm).

Table 1

Primers for real-time PCR

Gene	Forward	Reverse
GAPDH	5′-AAGCCTGCCGGTGACTAAC	5′-GTTAAAAGCAGCCCTGGTGAC
KLF2	5′-CAAGACCTACACCAAGAGTTCG	5′-CATGTGCCGTTTCATGTGC
Gapdh(rats)	5′-GCAAGTTCAACGGCACAG	5′-GCCAGTAGACTCCACGACAT
Klf2(rats)	5′-ACTTGCAGCTACACCAACTG	5′-CTGTGACCCGTGTGCTTG
Gapdh	5′-GCCATCAACGACCCCTTCAT	5′-ATGATGACCCGTTTGGCTCC
Klf2	5′-CCAGCCGGGAAATGGATACTGTC	5′-CCCTAACATTCTGAGATTAGGTCTG
Pecam-1	5′-AGCCTAGTGTGGAAGCCAAC	5′-AGCCTTCCGTTCTCTTGGTG
Icam-1	5′-CCGTGCAGTCGTCCGCTTCCG	5′-GGGTCCGCGGTGCTCCACCAT
Vegfa	5′-CTGGACCCTGGCTTTACTGC	5′-CTGCTCTCCTTCTGTCGTGG
Flt1	5′-TCAAGCTAGAGGTGTCCCCG	5′-CTCGGCACCTATAGACACCC
Kdr	5′-TACAAGTGCTCGTACCGGG	5′-TTGAAATCGACCCTCGGCAG
Angpt-1	5′-TCCCTCTGGTGAATATTGGC	5′-TGCTCTGTTTGCCTGCTGTC
Angpt-2	5′-AGAAGCAGCAGCATGACC	5′-TGCCACTGGTGGTGAGTCC
Tjp1	5′-TAGCACGGACAGTAGACACA	5′-ATGGAAGTTGGGGTTCATAG
Nos3	5′-AGCACCAGACCACAGGTGA	5′-GAGGGTGTCGTAGGTGATGC
Nphs1	5′-GTGCCCTGAAGGACCCTACT	5′-CCTGTGGATCCCTTTGACAT
Nphs2	5′-CTTGGCACATCGATCCCTCA	5′-CGCACTTTGGCCTGTCTTTG
Synpo	5′-CTTTGGGGAAGAGGCCGATTG	5′-GTTTTCGGTGAAGCTTGTGC
Wt1	5′-GAGAGCCAGCCTACCATCC	5′-GGGTCCTCGTGTTTGAAGGAA
Podocyxlin	5′-CCATAAGGCCAGATGAGGAA	5′-GATTCTCTTCACTGCCACCG